Ab initio molecular dynamics simulation of liquid $Al_{88}Si_{12}$ alloys

Songyou Wang
Department of Optical Science and Engineering, State Key Laboratory of Advanced Photonic Materials and Devices, Fudan University, Shanghai 200433, Peoples' Republic of China, and Ames Laboratory, U.S. Department of Energy and Department of Physics and Astronomy, Iowa State University, Ames, Iowa 50011

C. Z. Wang and Feng-Chuan Chuang
Ames Laboratory, U.S. Department of Energy and Department of Physics and Astronomy, Iowa State University, Ames, Iowa 50011

James R. Morris
Metals and Ceramics Division, Oak Ridge National Laboratory, Oak Ridge, Tennessee 37831-6115

K. M. Ho
Ames Laboratory, U.S. Department of Energy and Department of Physics and Astronomy, Iowa State University, Ames, Iowa 50011

(Received 6 August 2004; accepted 22 October 2004; published online 3 January 2005)

First-principles molecular dynamics simulations are carried out to study the structures, dynamics, and electronic properties of liquid $Al_{88}Si_{12}$ in the temperature ranging from 898 to 1298 K. The temperature dependence of static structure factors, pair correlation functions, and electronic density-of-states are investigated. The structural properties obtained from the simulations are in good agreement with the x-ray diffraction experimental results. © *2005 American Institute of Physics.* [DOI: 10.1063/1.1833355]

I. INTRODUCTION

Al–Si binary alloy is a eutectic system with the eutectic composition at Al-13 wt.% Si.[1] Silicon plays an important role in Al–Si alloy. Si doping in Al can reduce the thermal expansion coefficient, increase corrosion and wear resistance, and improve casting and machining characteristics of the alloy. These unique properties of Al–Si alloys have attracted much attention in materials science and industry. In particular, Al–Si alloys have been commercially used to produce engine blocks due to their high strength over weight ratio.[2]

The growth methods and properties of Al–Si alloys have been studied extensively by experiment.[3–10] Properties of liquid metals and alloys were shown to depend on growth methods and temperature, and melt overheating resulted in significant changes in the properties and structure of the liquids. It has been reported that melt overheating and quick cooling to a pouring temperature significantly modify the microstructure of Al–Si alloy without addition of modifying elements.[6–10] The structural properties of the liquid $Al_{88}Si_{12}$ alloys have been measured by Bian *et al.*[7] using x-ray diffraction at temperatures ranging from 898 to 1298 K. They found that the liquid structure changed by the thermal treatment at different temperatures. The atomic density, the coordination number, and the structure factor have a sudden change in the temperature range from 1048 to 1148 K. This change was interpreted as dissolving of Si–Si clusters into the Al bulk melt. Therefore, in the experiment the equilibrated liquid states are at the temperatures of 1148 K or higher and liquid Al–Si and Si clusters coexist below 1148 K.

Despite of a lot experimental effort devoted to the studies of liquid Al–Si alloys, the atomic structures and the relationship between the structures and properties of the liquids are still not well understood. Knowledge about the liquid structures and properties from atomistic simulations is therefore desirable. Due to the recent development of the *ab initio* molecular dynamics simulations, it is possible to study the atomic and electronic structure of liquid metals and alloys from the first-principles perspective.[11–15] Results from *ab initio* simulations have provided useful information for understanding the microscopic structure and properties of metallic liquids alloy.

In this paper, we describe a numerical study of $Al_{88}Si_{12}$ over a range of temperature using *ab initio* molecular dynamics simulations. The paper is organized as follows: In Sec. II, we summarize our approach and method of calculation. The results of the simulations are presented in Sec. III. Finally, a short summary is given in Sec. IV.

II. COMPUTATION METHOD

Our simulations were carried out using the Vienna *ab initio* simulation package (VASP).[16] The system consists of 44 Al atoms and 6 Si atoms in a cubic box with the periodic boundary conditions, which is corresponding to $Al_{88}Si_{12}$ alloys (or Al-13wt. %Si). We considered five temperatures with $T=898$, 948, 1048, 1148, and 1298 K, respectively. These temperatures are correspond to those in the experimental of Ref. 7, and are all above the melting point of the system. The atomic number densities at 1148 and 1298 K were taken from the experimental results.[7] As discussed in the previous section, in the experiment of Ref. 7, the liquids

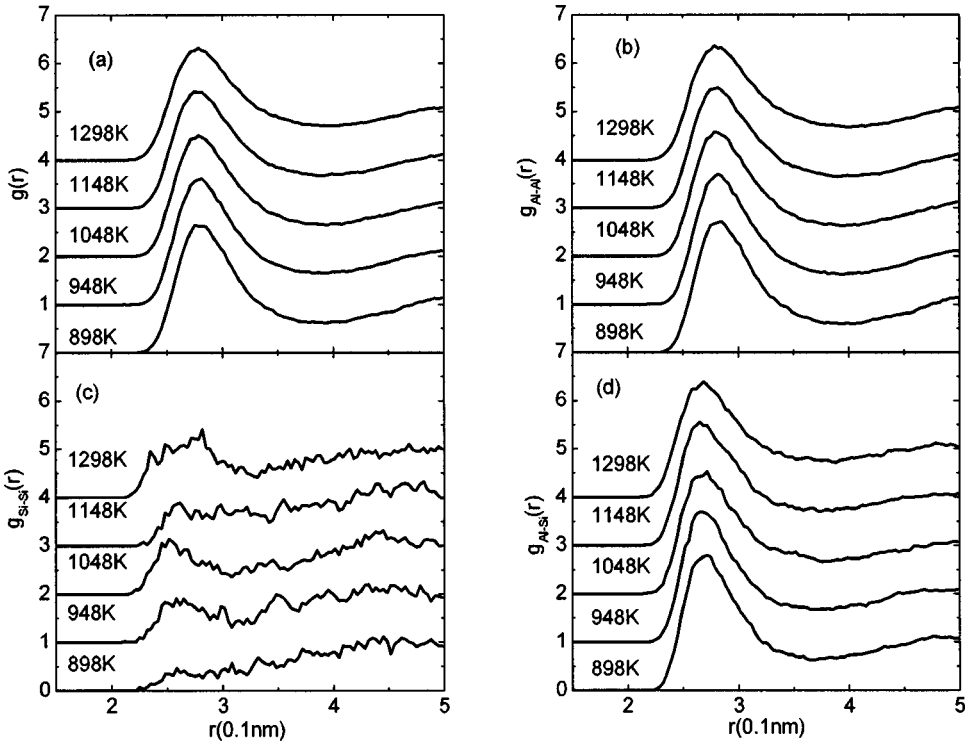

FIG. 1. Pair-correlation functions of $Al_{88}Si_{12}$ at different temperatures. (a) Total pair-correlation function; (b) partial pair-correlation function for Al–Al; (c) partial pair-correlation function for Si–Si; and (d) partial pair-correlation function for Al–Si. The graphs are vertically offset by one unit each for clarity.

reach equilibrium at these two temperatures. The density at the temperature lower than these two temperatures is determined by a linear interpolation using the two densities at 1148 and 1298 K. The atomic number densities that were used in our simulation are 0.04807, 0.04787, 0.04747, 0.04707, and 0.04647 atoms/Å^3, respectively, for the five different temperatures.

For a given ionic configuration, the total energy is calculated using first-principles density functional formalism. The force on each ion is calculated using the Hellmann–Feynman theorem. Then, Newton's equations of motion are integrated numerically for the ions, using a time step of 5 fs. We used the canonical ensemble where the ions temperature was controlled using the Nose–Hoover thermostat.[17] We used a plane-wave pseudopotential representation, with ultrasoft pseudopotentials for both Al and Si species and with a plane-wave energy cutoff of 150.5 eV.[16] The Γ-point sampling is used for the supercell Brillouin zone. Our simulations were performed using local-density approximation (LDA) for the exchange correlation energy.

In our iteration of Newton's law in liquid $Al_{88}Si_{12}$, we start with the 50 atoms in random positions in the cubic supercell. This starting configuration is allowed to iterate for 2000 time steps (10 ps) at a temperature of 1600 K. Then the system was cooled down to 1298 K at a uniform cooling rate for about 2.5 ps. The simulation was further carried out for another 2000 time steps (10 ps) to collect the configurations for statistical analysis of the structures and properties of the liquid. Based on the configuration of 1298 K, the system is further cooled down to 1148 K using the same procedure as discussed above to perform the simulation for 1148 K. This procedure is repeated for 1048, 948, and 898 K where the configuration at 1048 K is obtained by cooling from 1148 K, and so on.

III. RESULTS AND DISCUSSION

A. Structural properties

The pair correlation function g(r) is calculated from the relation

$$g(r)=\rho^{-2}\left\langle \sum_i \sum_{j\neq i} \delta(\mathbf{r}_i)\,\delta(\mathbf{r}_j-\mathbf{r}) \right\rangle. \tag{1}$$

Using the atomic coordinates from the molecular dynamics simulations, the total pair correlation functions g(r) are calculated and presented in Fig. 1(a) for liquid $Al_{88}Si_{12}$ at the different temperatures. As can be seen from Fig. 1(a), the first peak position of the total pair correlation function is around the 2.78 Å. The position of the first peak is not sensitive to the temperature. However, the peak heights decrease with increasing temperature.

The partial pair correlation functions $g_{\text{Al-Si}}(r)$, $g_{\text{Al-Al}}(r)$, and $g_{\text{Si-Si}}(r)$ can also be calculated when the density in Eq. (1) is set to be the corresponding partial density $\rho_{ij}=\rho\sqrt{c_i c_j}$, where ρ is the density of the system, i and j denote the elements in the alloy, and c_i and c_j are their concentrations. The partial pair correlation functions between the Al atoms, $g_{\text{Al-Al}}(r)$, for the liquid $Al_{88}Si_{12}$ at various temperatures are plotted in Fig. 1(b). The first peak in $g_{\text{Al-Al}}(r)$ is around 2.81 Å and exhibits very little shift with the temperature. This peak position is very close to that of the experimental value of 2.8 Å in pure liquid Al.[18] The height of the principal peak increases with decreasing temperature. The partial pair correlation functions for Si atoms, $g_{\text{Si-Si}}(r)$ at the different temperature, are shown in Fig. 1(c). The statistics for the $g_{\text{Si-Si}}(r)$ are not good because the number of Si atoms is too small, but the intensity of the first peak increasing as the temperature increases can be clearly seen. The $g_{\text{Si-Si}}(r)$

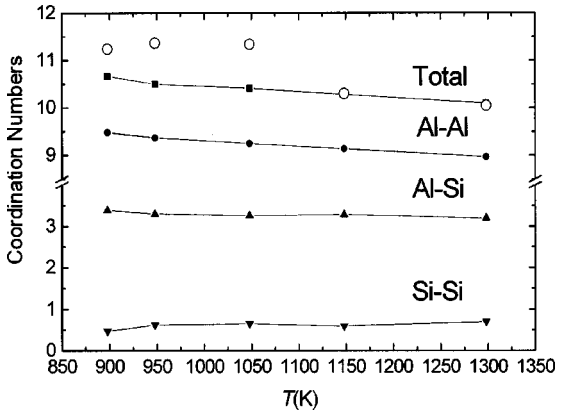

FIG. 2. Calculated coordination numbers as a function of temperature. For total coordination number, the squared line is present simulation and the opened circle is experiment.

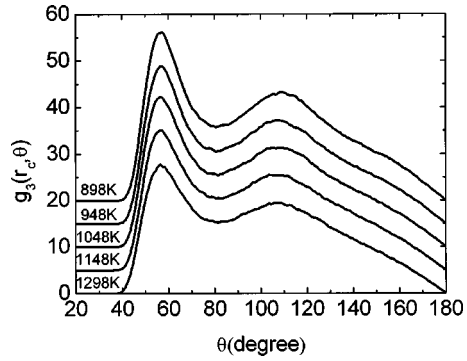

FIG. 3. Bond-angle distribution function of liquid $Al_{88}Si_{12}$ at different temperatures.

have a maximum around 2.5 Å, which is close to the experimental value 2.45 Å for pure liquid Si. These results suggest that Si atoms tend to form clusters when temperature increases. The partial pair correlation functions between Si and Al, $g_{\text{Al-Si}}(r)$, in liquid $Al_{88}Si_{12}$, are shown in Fig. 1(d). The shapes of $g_{\text{Al-Si}}(r)$ are similar to that of total g(r) at the corresponding temperature. The position of the first peak in $g_{\text{Al-Si}}(r)$ is 2.69 Å and there is almost no shift with temperature. But the height of the first peak in $g_{\text{Al-Si}}(r)$ increases with decreasing the temperature.

The microstructures of liquid can also be characterized by the average coordination number, which are obtained by integrating the $g_{\text{ij}}(r)$ to its first minimum,

$$N_{ij}=\int_0^{R_{\min}} 4\pi r^2 \rho_{ij} g_{ij}(r)\,\mathrm{d}r, \tag{2}$$

where $\rho_{ij}=\rho\sqrt{c_i c_j}$ is the partial number density of the atom as defined above. The bond length cutoff $R_{\min}$ is taken to be 3.73 Å in our calculation, which is the first minimum of the total pair correlation functions. The results are shown in Fig. 2. The average number of neighbors for liquid $Al_{88}Si_{12}$ alloys in the first shell is in the range of 10.7–10.1 and increases with decreasing temperature. The average coordination number obtained from our simulations is somewhat lower than the values found by Bian *et al.* in Ref. 7 for temperature below 1048 K. But the coordination numbers at 1148 K and 1298 K are in good agreement with the experimental results.[7] The partial coordination numbers for $N_{\text{Al-Al}}$ and $N_{\text{Al-Si}}$ decrease with increasing temperature, but $N_{\text{Si-Si}}$ increases with increasing temperature. These results are consistent with the pair correlation functions discussed above.

Information about the short-range order in the liquid alloy may also be obtained from bond angle distribution functions $g_3(r_c,\theta)$. This function is defined for angles between nearest neighbors atoms around a central atom with a maximum bond length r_c. Figure 3 gives $g_3(r_c,\theta)$ for liquid $Al_{88}Si_{12}$ at different temperature. The bond length cutoff is the same as that used in the calculation of coordination numbers as discussed above. The bond-angle distribution function shows two peaks, one around 56.5° and the other varies from 108.5° to 103.5°, decreasing with increasing the temperature. The peak height decreases with increasing temperature.

The quantity which is commonly measured by experiment for liquid is the total structure factor $S(k)$. Experimental probes usually measure the total structure factor $S(k)$, but can not directly separate the contributions of the partial components. In molecular dynamics simulations, it is possible to calculate not only the total structure factor but also the partial structure factor. If we know the appropriate scattering parameters, we can compare the results of total structure factor $S(k)$ obtained by calculations with that from experiment.

In theoretical calculation, $S(k)$ can be obtained using the results of three partial structure factor $S_{ij}(k)$ and the scattering lengths of the elements in the alloys from the following equation:

$$S(k)=\frac{\alpha_i^2 S_{ii}(k)+2\alpha_i\alpha_j S_{ij}(k)+\alpha_j^2 S_{jj}(k)}{\alpha_i^2+\alpha_j^2}, \tag{3}$$

where the ratio of neutron-scattering lengths for Al and Si is taken to be $\alpha_{\text{Al}}/\alpha_{\text{Si}}=3.449/4.1491$.[19] The partial structure factors can be calculated by Fourier transformation of the partial pair correlation functions $g_{ij}(r)$,

$$S_{ij}(k)=\delta_{ij}+4\pi\rho_{ij}\int_0^{\infty}[g_{ij}(r)-1]\frac{\sin(kr)}{kr}r^2\,\mathrm{d}r, \tag{4}$$

where i and j denote the two components of the binary alloy and ρ_{ij} is the same as that in Eq. (2). The total and partial structure factors obtained from our simulations are plotted in Fig. 4. The calculated total structure factors are compared with the x-ray diffraction data obtained by Bian *et al.*[7] at $T=1148$ and 1298 K as shown in Fig. 4(a). The agreement between the theory and experiment for the first and second peaks at 2.66 and 5.0 Å is quite good. The peak heights of the first and second peaks are found to decrease with increasing temperature. The statistics of the partial structure factor for Si are not good because the number of Si atoms is too small in the sample. The $S_{\text{Al-Al}}(k)$ has a similar shape as the total $S(k)$, the peak positions for the first and second peaks are at ~2.63 and ~4.85 Å^{-1} respectively, a little smaller than that of pure liquid Al which are 2.7 and 5.0 Å^{-1}. The structure factor between opposite pairs [Fig. 4(d)] is negative for small k, becoming positive at k values corresponding to

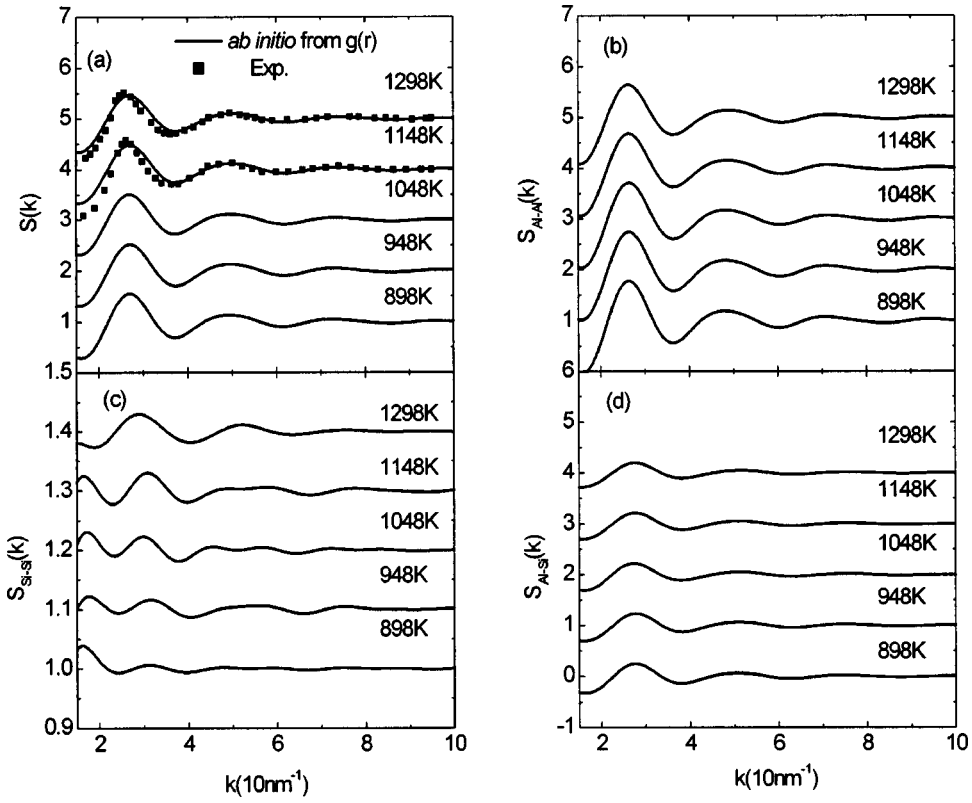

FIG. 4. Structure factors of $Al_{88}Si_{12}$ at different temperatures. (a) Total structure factor; (b) partial structure factor of Al–Al; (c) partial structure factor of Si–Si; and (d) partial structure factor of Al–Si. In (a), The line is *ab initio*; dotted is experiment. All the graphs are vertically offset one unit for clarity.

the peaks in the other two partial structure factors, and closes to zero for k bigger than 6 Å^{-1}. The first and second peak positions are at ~2.73 and ~5.05 Å^{-1}, respectively, and the peak heights increase with decreasing temperature.

Experimentally, the total pair correlation function $g(r)$ is obtained by Fourier transformation of the measured total structure factor $S(k)$. Therefore, the g(r) calculated from Eq. (1) cannot compare directly with experimental results because of the different scattering lengths for Al and Si. In order to compare with experiment, one can calculate g(r) using the calculated total structure factor $S(k)$ [see Eq. (3)] by a standard Fourier transformation technique,

$$g(r)=1+\frac{1}{2\pi^2\rho r}\int_0^{k_{\max}} k[S(k)-1]\sin(kr)dk. \qquad (5)$$

The calculated results for $g(r)$ from Eq. (5) at five temperatures together with the experimental results at $T=1148$ K and 1298 K are depicted in Fig. 5. The agreement between our calculated $g(r)$ and the experimental results is quite good. The peak position is at ~2.81 Å. The peak height from the calculation is slightly lower than that from experiment. Note that the peak height in Fig. 5 is lower than that in Fig. 1(a), because of the effects of the different scattering lengths for Al and Si which are considered in Fig. 5 but not in the calculation for Fig. 1(a). To compare with experiment, it is necessary to include the effects of the scattering lengths in $g(r)$.

In comparison with the simulation results of Ref. 15, our results are in better agreement with experiment. One of the reasons for such an improvement is that we use different neutron-scattering lengths (as determined by experiment, Ref. 19) for the two elements in the liquid when performing the analysis for the structure factors and pair correlation functions, while such difference in the scattering lengths is not considered in Ref. 15. Slight differences in the densities and temperatures may also contribute to the difference in the results from the two simulations.

B. Dynamical properities

The self-diffusion coefficient for Al and Si in liquid AlSi alloys can be extracted from the equation

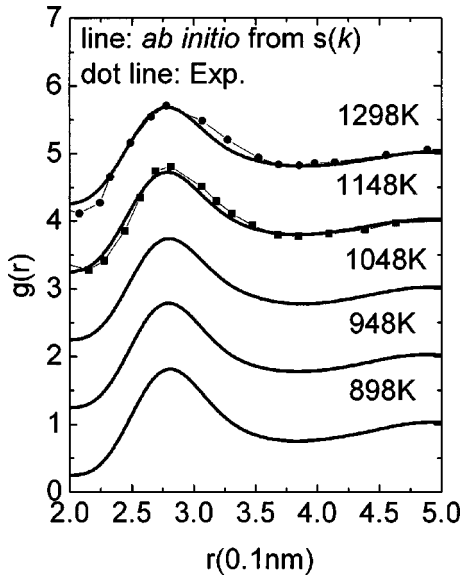

FIG. 5. Total pair-correlation functions for liquid $Al_{88}Si_{12}$ at different temperatures. The line is *ab initio*; dotted is experiment. The graphs are vertically offset by one unit each for clarity.

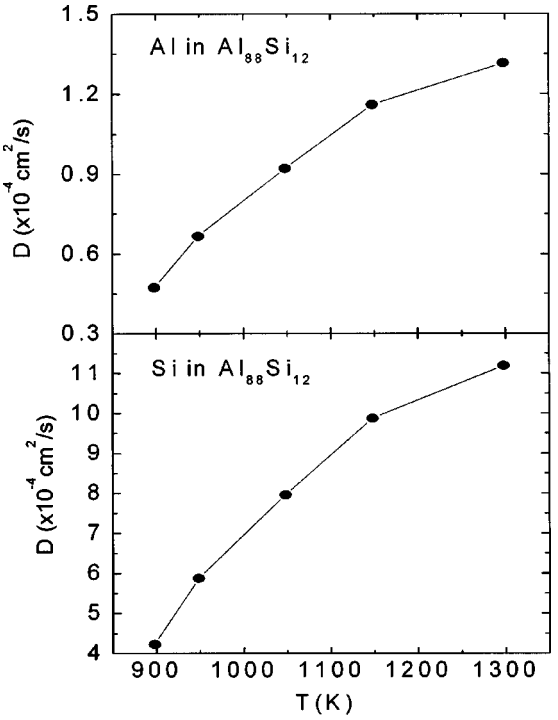

FIG. 6. Self-diffusion constant for Al and Si in liquid $Al_{88}Si_{12}$ at different temperatures.

$$D_\alpha = \lim_{t\to\infty} \frac{\langle |R_\alpha(t) - R_\alpha(0)|^2 \rangle}{6t}, \tag{6}$$

where $R_\alpha(t)$ denotes an ionic position of the α-type atom at time t. The angular brackets denote an average over all the ions of the same species and also over all time origin. The results for Al and Si in the liquid $Al_{88}Si_{12}$ alloys are shown in Fig. 6. For Al in the liquid $Al_{88}Si_{12}$, D_{Al} increases with increasing the temperature; the value is in the range from 0.47×10^{-4} to 1.31×10^{-4} cm^2/s. These values are similar to the previous theoretical results of $0.49-1.05\times10^{-4}$ cm^2/s for pure liquid Al in the temperature range of 943–1323 K.[20] For Si, D_{Si} has the same characteristic as D_{Al}, but the values are bigger than that of Al, ranging from 4.2×10^{-4} to 11.2×10^{-4} cm^2/s.

C. Electronic properties

The electronic density-of-states (DOS) of liquid $Al_{88}Si_{12}$ are calculated from the expression

$$N(E) = \sum_{\mathbf{k},E_\mathbf{k}} w_\mathbf{k} g(E - E_\mathbf{k}), \tag{7}$$

where $E_\mathbf{k}$ is the eigenvalues of the one-electron Hamiltonian at a particular k point of the supercell Brillouin zone and $w_\mathbf{k}$ is the weight of that k point. $g(E)$ is a Gaussian function with a width of 1.0 eV. The set of eight special k points in the supercell Brillouin zone is used in the present calculation.[21] Each k point has the same weights $w_\mathbf{k}$. For each k point we chose the lowest 150 eigenvalues $E_\mathbf{k}$, and the final density-of-states are then obtained by averaging over 15 representative configurations for each temperature. The Fermi energy is shifted to zero for the presentation. The calculation results

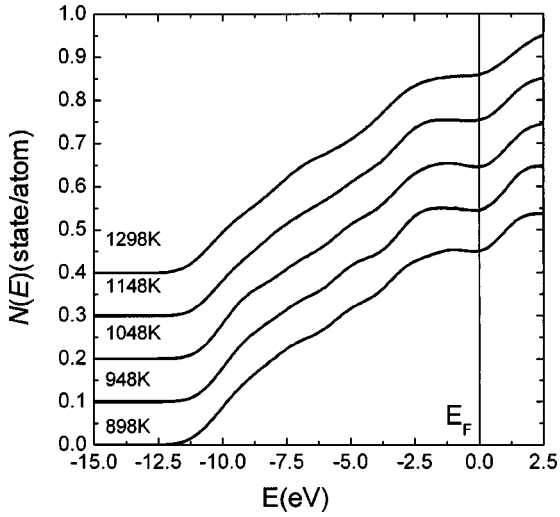

FIG. 7. Calculated electronic density of state $N(E)$ for liquid $Al_{88}Si_{12}$ at different temperatures.

are shown in Fig. 7 for $Al_{88}Si_{12}$ alloy at different temperature. The DOS of liquid $Al_{88}Si_{12}$ has the free-electron-like behavior for the temperature range studied in this paper. It is also interesting to note that there is a depression of the DOS at Fermi level in the liquid $Al_{88}Si_{12}$ alloy at lower temperature. The minimum at the Fermi level is more prominent at $T=1048$ K and vanishing with rising temperature. This feature was observed in experiments with photoelectron spectroscopy in Al–Ge,[22,23] Pb–Bi, and Ti–B liquid alloys.[24]

IV. CONCLUSIONS

In summary, we have simulated the structure of liquid $Al_{88}Si_{12}$ alloys at different temperatures using *ab initio* molecular dynamics. The pair correlation function, structure factor, diffusion constant and electronic density-of-state as a function of temperature have been studied. The calculated total pair correlation functions and structure factors at high temperature are in good agreement with the available experimental data. We found that the systems have the free-electron-like metallic features. The coordination number of the total Al–Al and Al–Si decrease with increasing the temperature but for Si the coordination number increases with increasing temperature, indicating that Si atoms tend to form clusters with increasing the temperature. Note that the clustering of Si atoms at high temperature is different from the persistence of Si clusters in the melt AlSi alloys at low temperature as observed in Ref. 7. In the experiment of Ref. 7, the liquid alloys were prepared from the mass mixing of Al and Si at the temperatures much lower than the melting temperature of Si (which is 1683 K). Therefore, some Si clusters may persist in the low-temperature liquids due to incomplete dissolving of Si clusters. The presence of Si clusters in Al–Si liquid below 1148 K is signaled by the sudden changes in the density and the peak height of the structure factor from 1048 to 1148 K as measured in the experiment. In our simulation, the liquid is prepared at a high temperature of 1600 K and then is cooled down to study the temperature dependence of

the structure and properties of the liquid. Therefore, the clustering tendency of Si at high temperature is likely to be a true effect.

ACKNOWLEDGMENTS

We would like to thank Dr. U. Dahlborg, Dr. M. Calvo-Dahlborg, Dr. D. Sordelet, and Dr. M. Kramer for useful discussions. Ames Laboratory is operated for the U.S. Department of Energy by Iowa State University under Contract No. W-7405-Eng-82. Oak Ridge National Laboratory is operated for the U.S. Department of Energy under contract DE-AC05-00OR-22725 with UT-Battelle, LLC. This work was supported by the Director for Energy Research, Office of Basic Energy Sciences including a grant of computer time at the National Energy Research Supercomputing Center (NERSC) in Berkeley. This work is also supported by National Natural Science Foundation of China under Grant Nos. 60028403 and 60327002.

[1] T. B. Massalski, H. Okamoto, P. R. Subramanian, and L. Kacprzak, *Binary Alloy Phase Diagrams* (ASM International, Materials Park, OH, 1990).
[2] H. Ye, J. Mater. Eng. Perform. **12**, 288 (2003).
[3] B. Bokhonov and M. Korchagin, J. Alloys Compd. **312**, 238 (2000).
[4] P. Li, V. I. Nikitin, E. G. Kandalova, and K. V. Nikitin, Mater. Sci. Eng., A **332**, 371 (2002).
[5] R. Qin and E. R. Wallach, Mater. Trans., JIM **44**, 968 (2003).
[6] X. F. Bian and J. Ma, Chin. J. Mech. Eng. **51**, 76 (1992).
[7] X. F. Bian and W. Wang, Mater. Lett. **44**, 54 (2000).
[8] W. M. Wang, X. F. Bian, H. R. Wang, Z. Wang, L. Zhang, Z. G. Liu, and J. M. Liu, J. Mater. Res. **16**, 3592 (2001).
[9] K. Kristiakova, P. Svec, J. Kristiak, P. Duhaj, and O. Sausa, Mater. Sci. Eng., A **226–228**, 321 (1997).
[10] H. Chiriac, F. Vinai, M. Tomut, A. Stantero, and E. Ferarra, J. Non-Cryst. Solids **250–252**, 709 (1999).
[11] R. V. Kulkarni and D. Stroud, Phys. Rev. B **62**, 4991 (2000).
[12] R. V. Kulkarni and D. Stroud, Phys. Rev. B **57**, 10476 (1998).
[13] L. Vočadlo, D. Alfè, G. D. Price, and M. J. Gillan, Phys. Earth Planet. Inter. **120**, 145 (2000).
[14] C. Massobrio, A. Pasquarello, and R. Car, Phys. Rev. B **64**, 144205 (2001).
[15] M. Ji and X. G. Gong, J. Phys.: Condens. Matter **16**, 2507 (2004).
[16] G. Kresse and J. Hafner, Phys. Rev. B **47**, 558 (1993); G. Kresse, Ph.D. Technische Universität Wien, 1993; G. Kresse and J. Furthmüller, Comput. Mater. Sci. **6**, 15 (1996); G. Kresse and J. Furthmüller, Phys. Rev. B **54**, 11169 (1996); G. Kresse and J. Joubert, *ibid.* **59**, 1758 (1999).
[17] S. Nosé, J. Chem. Phys. **81**, 511 (1984); W. G. Hoover, Phys. Rev. A **31**, 1695 (1985).
[18] http://www.iamp.tohoku.ac.jp/database/scm/LIQ/gr.html
[19] National Nuclear Data Center at Brookhaven National Lab, Neutron News **3**, 29 (1992).
[20] D. J. González, L. E. González, J. M. López, and M. J. Stott, Phys. Rev. B **65**, 184201 (2002).
[21] J. M. Holender, M. J. Gillan, M. C. Payne, and A. Simpson, Phys. Rev. B **52**, 967 (1995).
[22] B. Grosdidier and J. G. Gasser, J. Non-Cryst. Solids **250–252**, 309 (1999).
[23] R. Gampp, F. Baumann, H.-G. Boyen, A. Cossy-Favre, G. Gantner, P. Oelhafe, and P. Häussler, J. Non-Cryst. Solids **156–158**, 236 (1993).
[24] P. Häussler, G. Indlekofer, H.-G. Boyen, P. Oelhafe, and H.-J. Güntherodt, Europhys. Lett. **15**, 759 (1991).